Mapping of power consumption and friction reduction in piezoelectrically-assisted ultrasonic lubrication

Sheng Dong, Marcelo J. Dapino

NSF I/UCRC on Smart Vehicle Concepts,
Department of Mechanical and Aerospace Engineering,
The Ohio State University, Columbus, OH 43210, USA

ABSTRACT

Ultrasonic lubrication has been proven effective in reducing dynamic friction. This paper investigates the relationship between friction reduction, power consumption, linear velocity, and normal stress. A modified pin-on-disc tribometer was adopted as the experimental set-up, and a Labview system was utilized for signal generation and data acquisition. Friction reduction was quantified for 0.21 to 5.31 W of electric power, 50 to 200 mm/s of linear velocity, and 23 to 70 MPa of normal stress. Friction reduction near 100% can be achieved under certain conditions. Lower linear velocity and higher electric power result in greater friction reduction, while normal stress has little effect on friction reduction. Contour plots of friction reduction, power consumption, linear velocity, and normal stress were created. An efficiency coefficient was proposed to calculate power requirements for a certain friction reduction or reduced friction for a given electric power.

Keywords: ultrasonic lubrication, piezoelectric actuator, friction reduction, power consumption

1. INTRODUCTION

Friction is the resistance to the motion between two contacting surfaces that slide or roll relative to each other.[1] By superimposing ultrasonic vibrations to the macroscopic velocity, dynamic friction can be reduced. This phenomenon is often referred to as ultrasonic lubrication. It is within the regime of high power applications of ultrasonics, where ultrasonic vibrations change the physical properties of materials.[2] Ultrasonic vibrations are usually generated by piezoelectric materials, which are a class of "smart" ceramics that can be used as solid-state actuators or sensors.

Ultrasonic lubrication has been known for decades and has been implemented in many industrial applications.[3] For example, in metal machining and forming processes such as drilling, pressing, sheet rolling, and wire drawing, ultrasonic vibrations have been utilized to reduce the force between tool and workpiece, replacing costly and environmentally aggressive oils and leading in all cases to improved surface finish.[4] In vehicles, ultrasonic lubrication can be integrated to suspension joints to automatically adapt themselves to various road conditions. In consumer product, the reduction of friction between the product and human skin can greatly enhance the user's experience. In space vehicles, where traditional lubricants cannot be used, ultrasonic lubrication can help reducing wear and extending the life of critical components.

2. BACKGROUND

Ultrasonic vibrations are usually applied only to one of the two contacting surfaces and may be applied in one of three directions relative to the macroscopic sliding velocity: perpendicular, longitudinal or transverse. Numerous studies have been devoted to each of the three directions and combinations thereof. Figure 1 shows a summary of the friction reduction results of the experiments conducted in all three directions. Friction reduction percentages are plotted against two other critical parameters that could influence the effectiveness of ultrasonic lubrication: normal stress and linear velocity.

Further author information: (Send correspondence to M.J.D.)
M.J.D.: E-mail: dapino.1@osu.edu, Telephone: 1 614 688 3689
S.D.: E-mail: dong.121@osu.edu, Telephone: 1 614 736 1818

Industrial and Commercial Applications of Smart Structures Technologies 2015,
edited by Kevin M. Farinholt, Steven F. Griffin, Proc. of SPIE Vol. 9433, 943304
 · doi: 10.1117/12.2085567

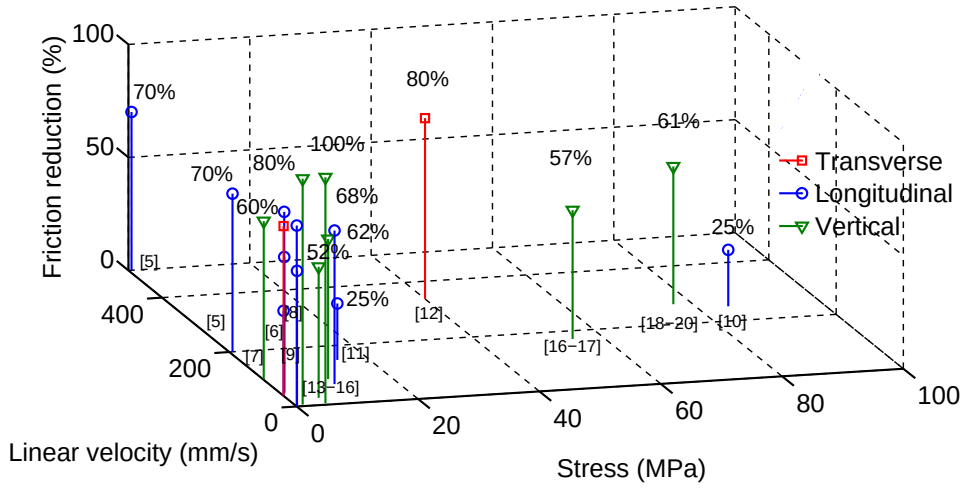

Figure 1. Map of ultrasonic friction reduction, linear velocity, and normal stress from literature.

For example, Littman et al.[5] used a piezoelectric actuator generating vibrations at 60 kHz, making it slide longitudinally on a guide track. The sliding velocity ranged from 0 to 0.5 m/s, and the velocity of the ultrasonic vibration was up to 0.26 m/s. They achieved friction reduction up to 70%, and found that friction reduction decreases as the velocity increases. Kumar and Hutchings[6] experimentally studied the influence of in-plane longitudinal and transverse vibrations on friction reduction at low normal stresses. A pin-on-disc set-up was employed, where the pin was made of aluminum, copper, and stainless steel while the disc was held by a table with reciprocating motion. They determined that longitudinal vibrations were more effective at reducing friction force than transverse vibrations.

Popov et al.[7] studied ultrasonic friction reduction under low loads and low velocities for different material combinations using a pin-on-disc tribometer. It was shown that ultrasonic vibrations create less friction reduction on softer materials than harder ones. They argued that contact stiffness influences the degree of friction force reduction. Teidelt et al.[8] extended the work of Popov et al.[7] using the same experimental set-up, but they applied ultrasonic vibrations in the vertical direction. They varied the vibrational amplitude and reached friction reduction up to 60%. Gutowski and Leus[9] measured friction force between a slider and a base with and without longitudinal ultrasonic vibrations applied to the base. The normal stress (0.031 MPa) and linear velocity (0.62 mm/s) were set at low range. Friction reduction up to 90% was achieved by increasing the vibrational velocity to 6.64 mm/s, which is more than ten times the macroscopic velocity.

Pohlman and Lehfeldt[10] managed to reduce drawing force by 25% during wire drawing processes. They also conducted similar ball-on-disc experiments by applying ultrasonic vibrations in tangential, transverse, and vertical directions relative to the macroscopic sliding velocity. Unlike other studies, they used a magnetorestrictive transducer for generating ultrasonic vibrations. Also, they employed Molykote as the lubricant to treat the surfaces before applying ultrasonic vibrations. Oiwa[11] studied the influence of ultrasonic vibrations on rolling friction. Tests were conducted on linear-motion guides for precision positioning, the accuracy of which may have been substantially reduced by the presence of friction and the resulting stick-slip phenomenon caused by it. Both the rail and the carriage were ultrasonically excited in the tests, and an overall 25% friction reduction was achieved. It was also reported that the reduction of static friction can only be reduced at a very low velocity. Tsai et al.[12] studied ultrasonic friction reduction using vibrations applied in angles with the macroscopic velocity. They concluded that vibrations in longitudinal direction are more effective than those in transverse direction.

Bharadwaj and Dapino[13–15] developed experiments in which longitudinal vibrations were used to investigate the effect of macroscopic sliding velocity, normal load, contact stiffness, and global stiffness on friction reduction. They experimentally demonstrated a decrease of up to 68% in effective friction coefficient. They also experimentally investigated ultrasonic lubrication for creating adaptive seat belts with controllable force at the interface

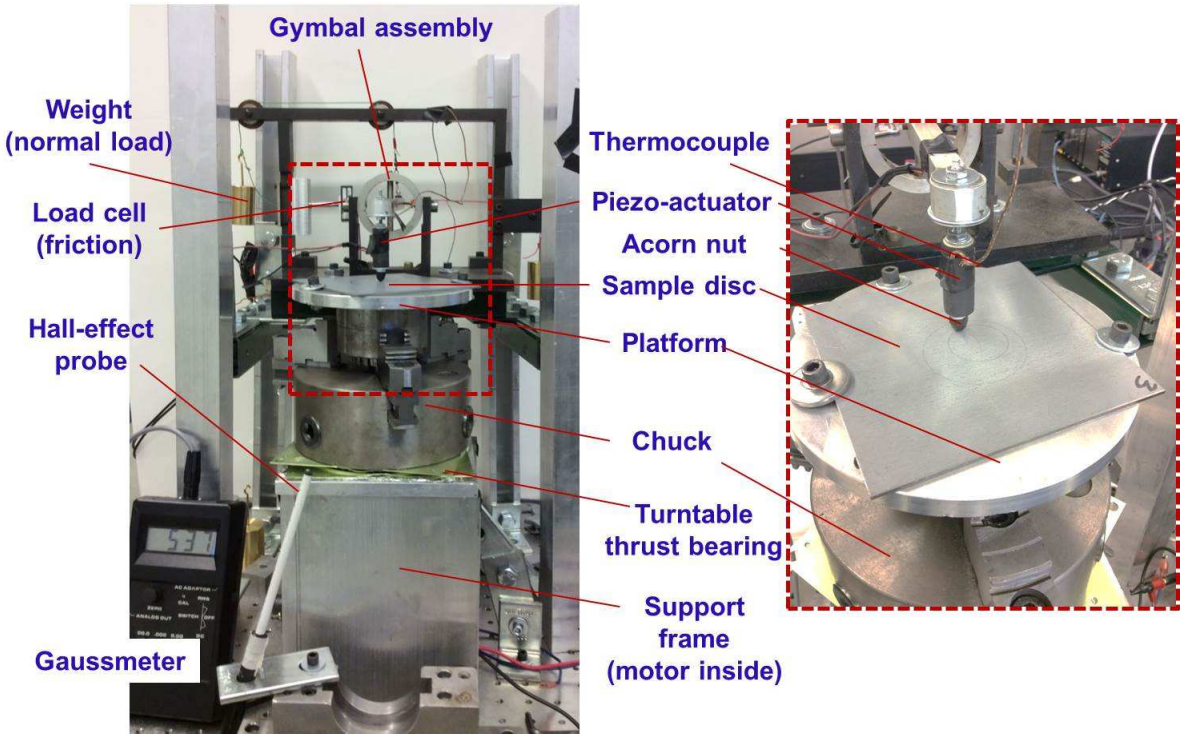

Figure 2. Experimental set-up.

between the D-ring and webbing. Proof-of-concept experiments were conducted under normal loads up to 670 N by using out-of-plane ultrasonic vibrations. Friction was reduced by up to 60%. Dong and Dapino[16–20] used the Poisson effect to generate vibrations in combined perpendicular and longitudinal directions relative to the overall sliding direction, and studied the relationship between friction reduction and normal load, contact materials, and global stiffness. They also conducted experiments to investigate ultrasonic friction and wear reduction using a modified pin-on-disc tribometer. They found up to 62% friction reduction and 48% wear reduction with velocity up to 87 mm/s and 4 MPa of normal stress.

Previous experiments have been conducted with various normal stresses and velocities, and different levels of friction reduction have been achieved. In this paper, we investigate the relationship between friction reduction, electric power, linear velocity, and normal stress, which has not been simultaneously addressed previously.

3. EXPERIMENTAL SETUP

Experimental set-up is shown in Fig. 2. A pin-on-disc tribometer was modified for this experiment by addition of a piezoelectric actuator. The actuator consists of a stack of ring-shape piezoelectric wafers. A through rod and fasteners are utilized to apply compression to the wafers to avoid tension. The pin, which consists of the actuator and an acorn nut, is connected to the arm of a gymbal assembly. The other end of the gymbal arm is connected to a weight through pulleys, which is employed to apply normal force at the interface. The pin is placed in contact with a 4.8 in. by 4.8 in. square plate, which is clamped on a platform. The platform is held by a chuck and connected to a DC motor through a splined shaft. The weight of the plate, the platform, and the chuck is supported by a frame via a turntable thrust bearing. The DC motor with controllable speeds is used to rotate the plate.

A load cell is installed on the gymbal assembly, pretensioned by a weight, and used to measure the friction force. A Hall-effect probe is placed next to the turntable and connected to a gaussmeter. A magnet is fixed at the rim of the turntable and creates peaks in the gaussmeter readings when it gets closest to the Hall-effect probe during the rotation. Time-dependent gaussmeter readings provide information of the number of the rotations during the test and the duration of each rotation.

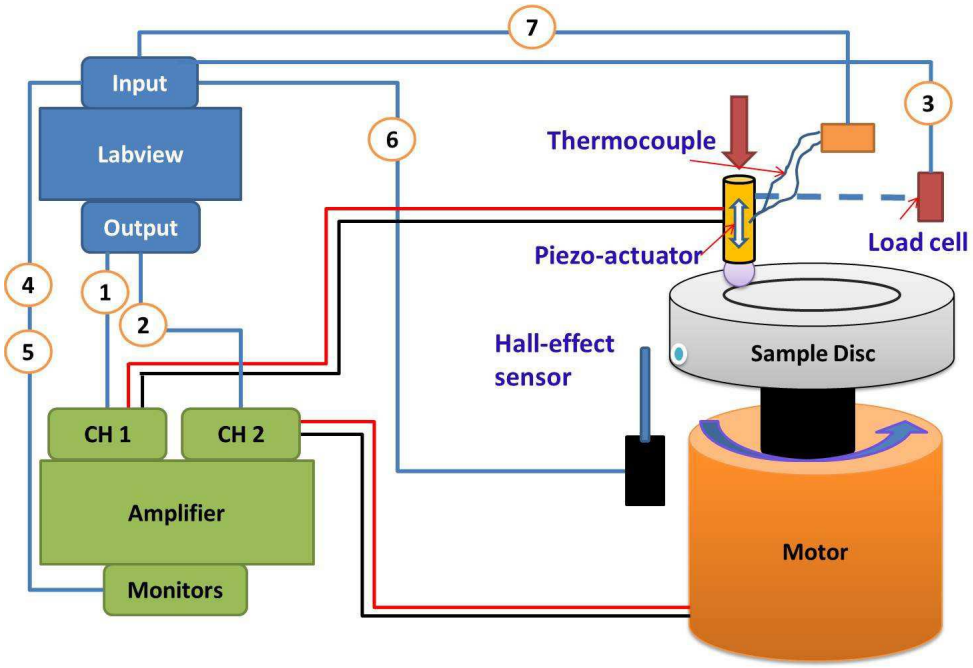

Figure 3. Connection diagram of the set-up.

Connection diagram of the experimental set-up is shown in Fig. 3. A Labview system was adopted for signal generation and data acquisition. An electrical amplifier magnifies the signals from the Labview and provides them to the actuator and the motor. An AC voltage with adjustable magnitudes (signal 1) is applied to the piezo-actuator to generate vibrations with different amplitudes, while a DC voltage (signal 2) is applied to drive the motor and control the rotational velocity. The data that the Labview system collects includes voltage and current applied to the piezo-actuator (signals 4 and 5), friction force measured by the load cell (signal 3), temperature of the actuator measured by a thermocouple (signal 7), and Hall-effect gaussmeter readings (signal 6).

Parameters used in this experiment are listed in Table 1. Normal load is set to be in the range of 3 N to 9 N with increments of 1 N. Nominal contact area is 0.126 mm^2 which is calculated from the width of the wear grooves. Correspondingly, nominal normal stresses are between 23 MPa to 70 MPa. Rotational velocity is controlled by the voltage that drives the motor. The voltage remains constant during each test and varies from test to test to reach various rotational velocities. Two rotational diameters, 1.1 in. (28 mm) and 1.9 in. (48.3 mm), are also adopted for different linear velocities. As a result, tests with six rotational velocities are conducted with each

Table 1. Parameters used in the experiment.

Parameter	Value
Normal load (N)	3, 4, 5, 6, 7, 8, 9
Nominal contact area (mm^2)	0.126
Nominal normal stress (MPa)	23, 32, 40, 48, 55, 63, 70
Rotational diameter (mm)	28, 48.3
Linear velocity (mm/s)	50-200
Peak-to-peak voltage (V)	0, 5.1, 10.3, 15.5, 20.7, 25.9
Actuator capacitance (nF)	360
Power consumed by the actuator (W)	0, 0.21, 0.84, 1.9, 3.39, 5.31
Nominal US amplitude (μm)	0, 0.46, 0.92, 1.38, 1.85, 2.31
US frequency (kHz)	22
Material	Uncoated steel for pin and disc

rotational diameter. Seven plates are prepared with each of them assigned for one normal load. Therefore, each wear scar can be created by the same amount of interaction between the pin and the plate. Piezo-actuator is driven at five levels of peak-to-peak voltages at 22 kHz, which is the resonance frequency of the actuator. The average power that drives the actuator is calculated as

$$P_a = CU_{max}U_{pp}f, \tag{1}$$

where C is the capacitance, f is the frequency, U_{max} is the maximum voltage, and U_{pp} is the peak-to-peak voltage. The corresponding power consumed by the actuator is between 0.21 W and 5.31 W, as listed in Table 1.

4. EXPERIMENTAL DATA

Representative results

The measurements of an example test are shown in Fig. 4. The test was conducted under 5 N of normal force and the rotational diameter was 1.1 in. Left figure plots the measured friction force against the time, while the right plot is the time-dependent voltage that drives the actuator (blue) and the reading from the gaussmeter (green). The test lasts for approximately 32.5 s and the motor starts rotating at 0.5 s. During the first 12 s of the test, the piezo-actuator is turned off so that the intrinsic friction can be measured. Ultrasonic vibrations are applied starting at 12.5 s, and five levels of voltages are employed, with 4 s duration for each. Average time intervals between two peaks is 1.34 s, therefore, linear velocity in this measurement is 65.5 mm/s.

As shown in the friction measurement, the intrinsic friction overcomes the static friction as the rotation initiates, which is around 1.2 N, to become dynamic friction. There exists fluctuation in the dynamic friction, which is due to the wobbling of the plate during the rotation. The intrinsic friction is 0.89±0.04 N at steady state. Friction is reduced when ultrasonic vibrations are applied, and remains at relatively constant levels despite the fluctuation. Friction drops 0.3 N with the initial application of 5.1 V voltage to the actuator. As the voltage increases, friction continues to decrease to greater extents. Friction reduction percentage is defined as

$$P_t = \frac{F_{t0} - F_{t1}}{F_{t0}} \times 100\%, \tag{2}$$

where F_{t0} is the intrinsic friction and F_{t1} is the friction force with ultrasonic vibrations applied. Table 2 lists the representative results of friction forces and reduction percentages. At the highest voltage (25.9 V), friction force is reduced to a very low level. Dong and Dapino[16] observed that, in some cases, the degree of friction reduction surpassed 100%. This was attributed to a "motor effect" created by the pizoelectrically induced vibrations.[21] In this study, friction reduction of 100% (and higher) were measured. Although it is not physically possible for the friction force to be negative, an experimental artifact is created when the string that connects the gymbal arm to the load cell is not taut during the measurements. This happens when the friction force is very low. It is then concluded that the amount of friction reduction at low speeds can be close to 100%.

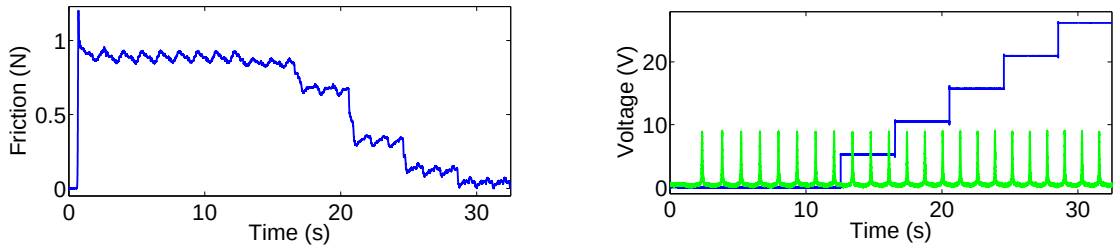

(a) (b)

Figure 4. Representative results: (a) friction force; (b) voltage (blue) and guassmeter reading (green).

Table 2. Representative results of friction and reduction percentage.

Voltage (V_{pp})	0	5.1	10.3	15.5	20.7	25.9
Friction (N)	0.89±0.04	0.85±0.03	0.67±0.04	0.32±0.04	0.12±0.04	0.04±0.04
Reduction (%)	N/A	2.60±1.49	25.36±0.83	66.94±2.45	90.49±3.47	100±3.87

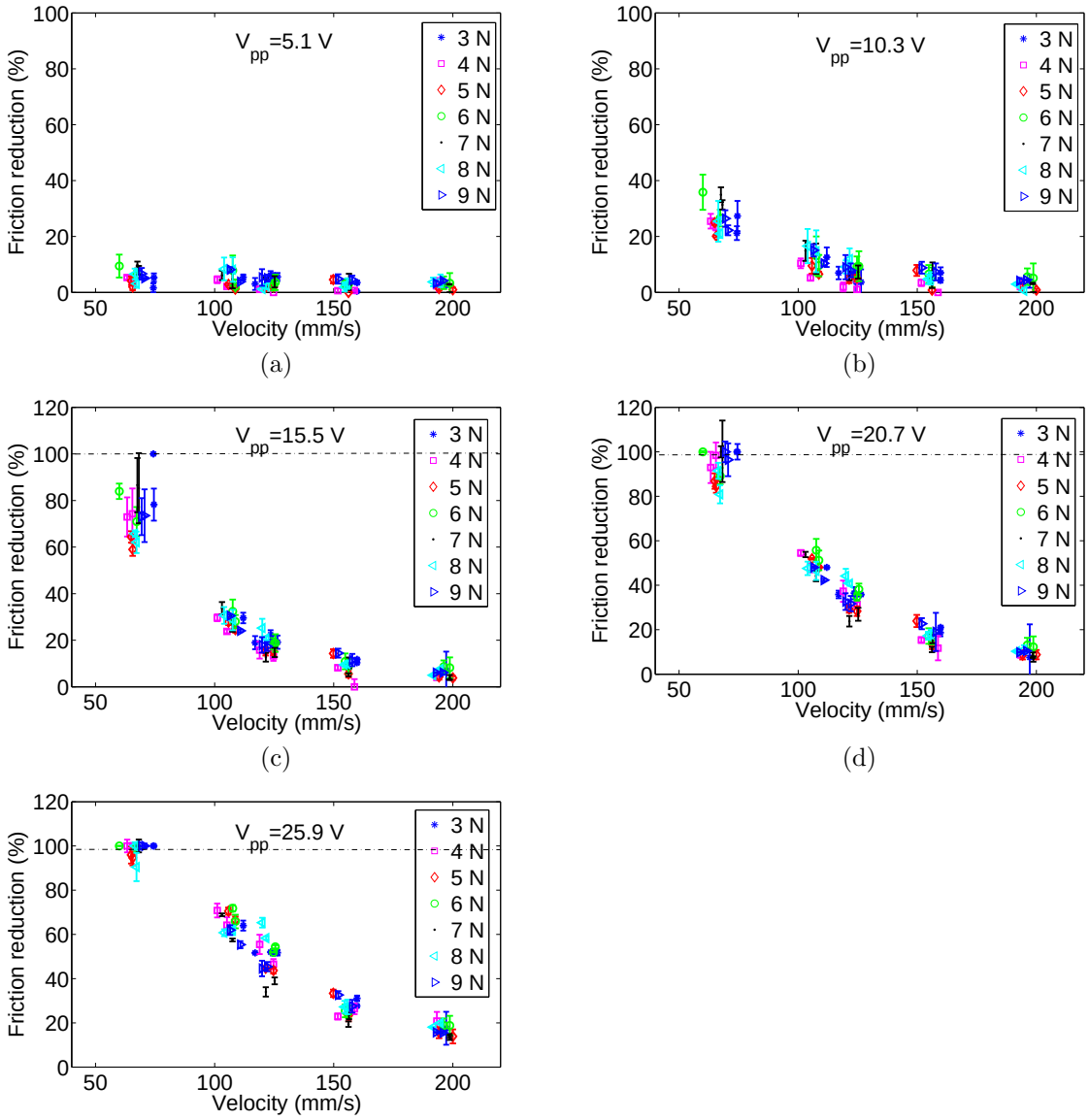

Figure 5. Relationship between friction reduction and linear velocity for five applied voltages.

Friction reduction vs. linear velocity

Tests were conducted following the format of the example test with various normal loads and linear velocities, as listed in Table 1. The reduction percentages are plotted against linear velocity in Fig. 5. Five plots represent five voltages applied, and various loads are denoted by different markers in each plot. At the lowest voltage (5.1 V), ultrasonic vibrations reduce friction by less than 10% for all linear velocities (Fig. 5(a)). As voltage increases to (10.3 V), friction reduction is improved, however, more reduction is achieved at lower velocities than higher velocities (Fig. 5(b)). A clear trend can be observed that higher velocities lead to lower friction reduction. At even higher voltages (15.5 V to 25.9 V), friction reduction continues to improve, and very low levels of friction are achieved at low velocities (Fig. 5(c)-(e)). Although lower velocity results in higher friction reduction, the relationship between reduction and velocity is not linear. Friction reduction drops faster at higher velocities.

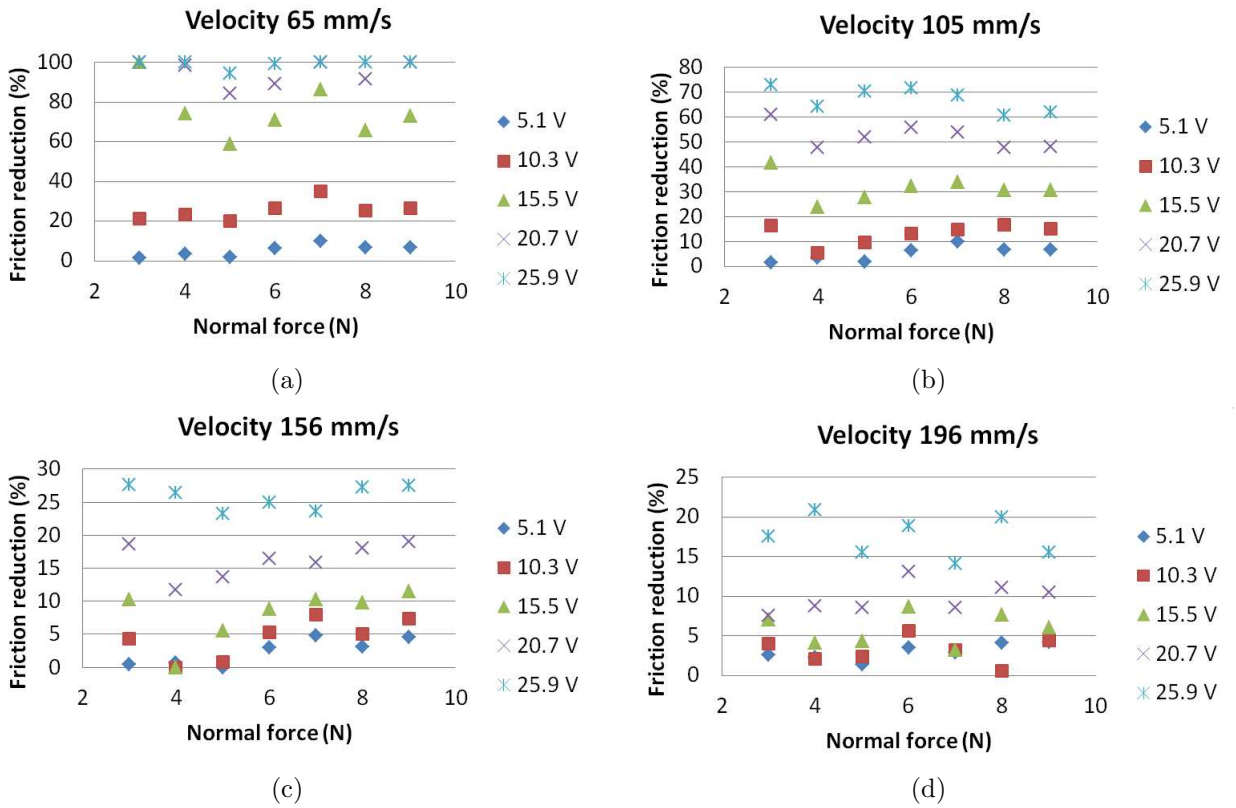

Figure 6. Relationship between friction reduction and normal load at four linear velocities.

Friction reduction vs. normal force

The relationships between friction reduction and normal force are plotted in Fig. 6. Each plot shows the data from one linear velocity, and five levels of voltages are represented by different markers.

The relationship between friction reduction and normal force appears relatively flat for most tests. However, there are variations in the curves, with friction reduction peaking at around 6 N or 7 N. This can be explained using the system dynamics of the modified tribometer. As described previously, different weights are connected to the gymbal assembly to apply normal forces. The arm of the gymbal assembly vibrates when ultrasonic vibrations are applied, which affects the total vibrations at the interface. The vibrational amplitude of gymbal arm changes as different weights (masses) are connected to the gymbal arm.

Higher amplitude of vibration is created at the gymbal arm when weights for 6 N and 7 N normal forces are connected. Although this type of vibration has much lower frequency (around 100 Hz) than the ultrasonic vibrations, it creates additional vertical movement between the pin and the plate, which leads to extra friction reduction. In this experiment, the extra friction reduction is less than 10%, which is not significant. However, this finding is meaningful to ultrasonic lubrication systems design. By carefully choosing the mass and stiffness of the system to match the resonance, the extra friction reduction can be achieved at much higher levels.

In summary, normal stress/load has little influence on ultrasonic friction reduction. However, the structure of the ultrasonic lubrication system may result in extra friction reduction.

Contour plots

Contour plots of friction reduction, linear velocity and normal stress are created by interpolating raw experimental data, shown in Fig. 7. At low voltage, there is no clear dependence of friction reduction (Fig. 7(a)). As voltage increases, the dominating influence of friction reduction is from linear velocity, although normal stress creates

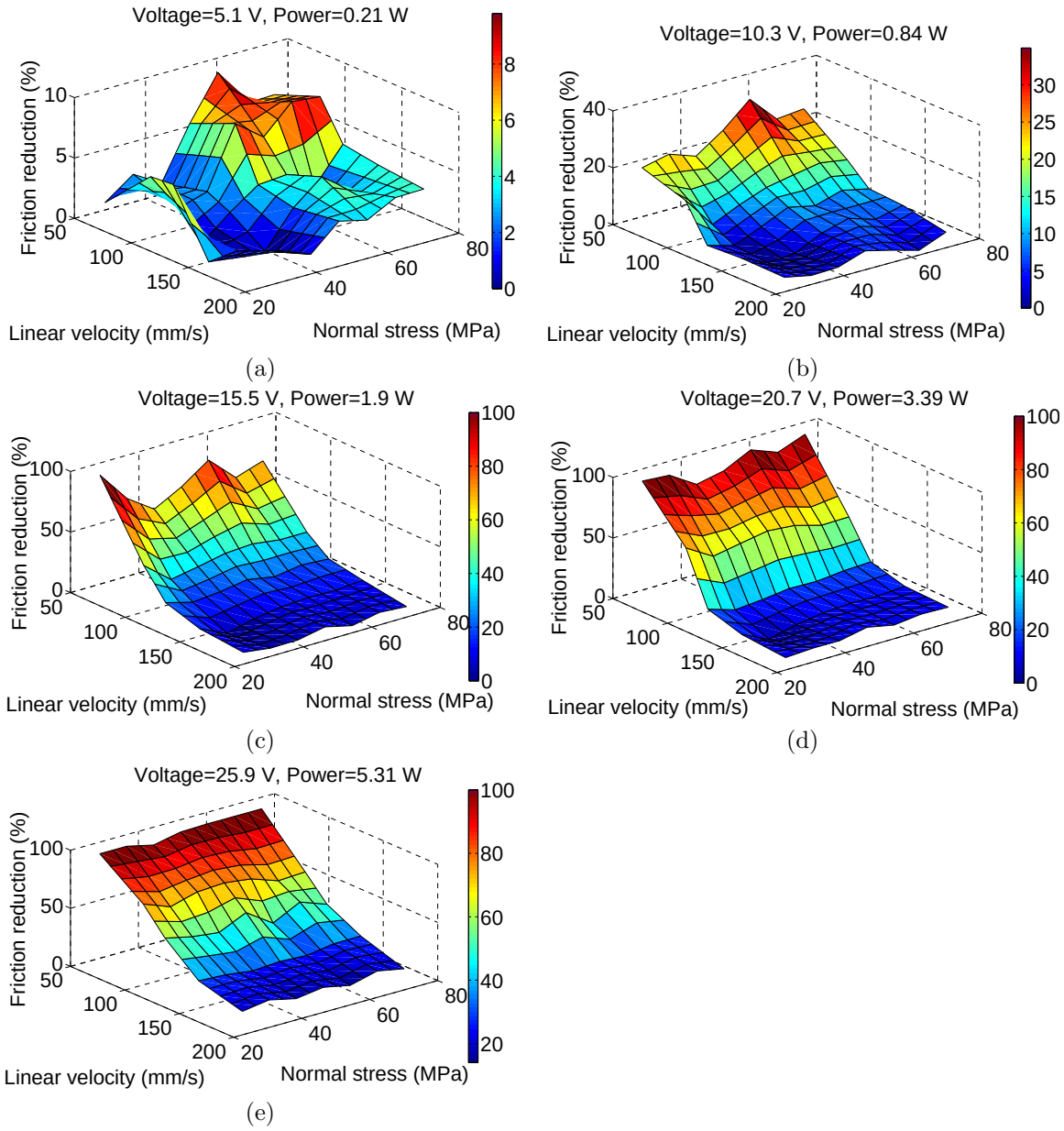

Figure 7. Contour plots of friction reduction, linear velocity, and normal stress for five power consumption levels.

variations (Fig. 7(b)-(e)). From a design point of view, if an ultrasonic lubrication system is driven at a certain voltage, there exists an optimum friction reduction in terms of the combination of stress and velocity.

Contour plots of friction reduction, power consumption, and linear velocity with various normal stresses are created, as shown in Fig. 8. The plots have similar shapes: greater friction reduction takes place at the lowest velocity when power is higher; lower friction reduction is either at higher velocity or with lower power. Neither of those two parameters are dominating the effect of friction reduction.

Same amount of friction reduction can be achieved at a high velocity with higher power or at a low velocity with lower power. To achieve better friction reduction, a trade-off exists between lowering the relative velocity between contacting surfaces and increasing the driving power of the ultrasonic lubrication component. At low velocities, there is an optimum power level where friction can be reduced to its minimum and remain at a low level. In that case, the extra power consumed does not create additional friction reduction.

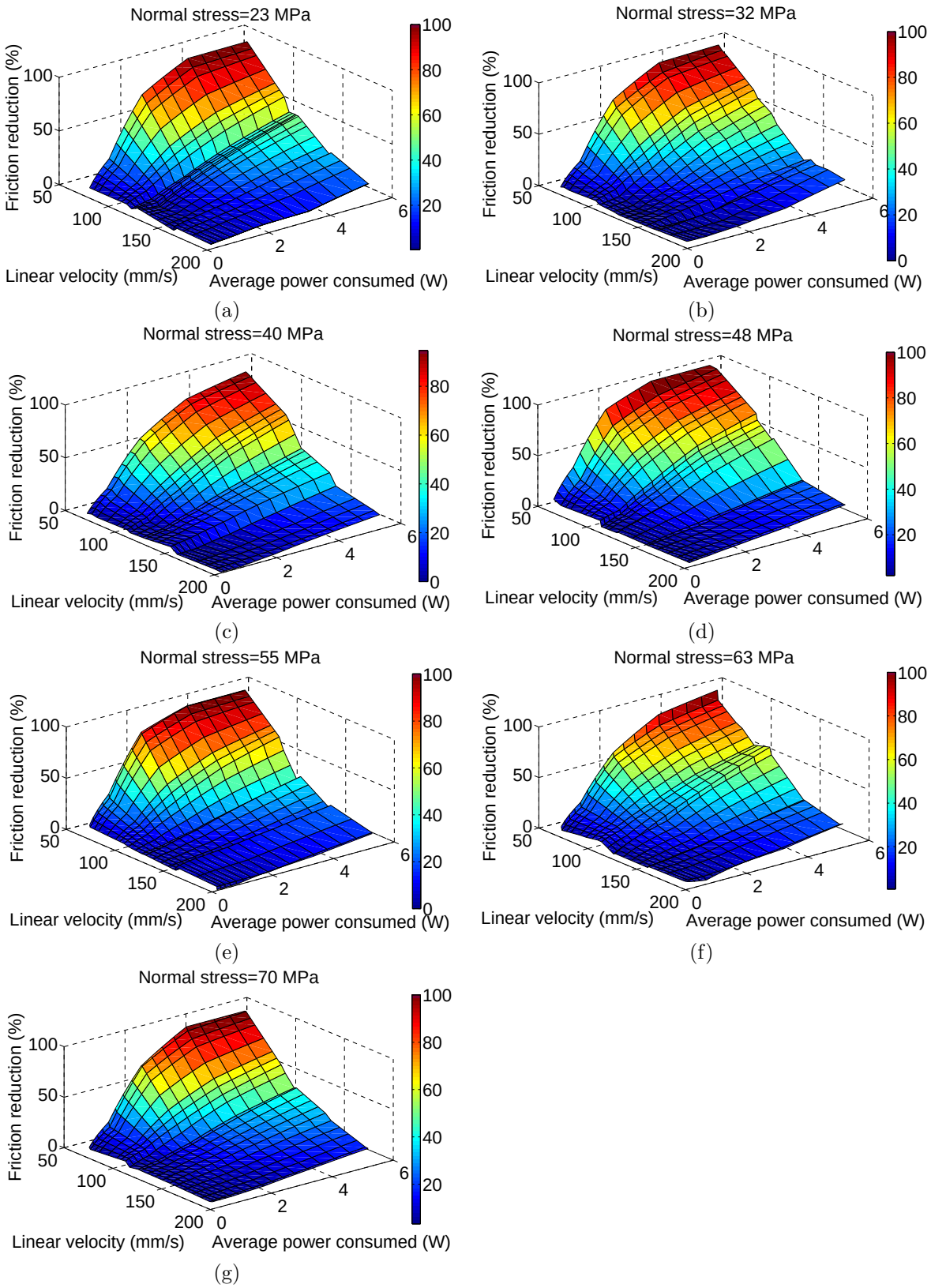

Figure 8. Contour plots of friction reduction, linear velocity, and power consumption for seven normal stress levels.

5. POWER, ENERGY, AND EFFICIENCY METRICS

An efficiency coefficient is proposed to utilize the information derived from the contour plots, which is defined as

$$\eta = \frac{(F_{t0} - F_{t1})v_{rel}A_n}{F_N P_a}, \tag{3}$$

where v_{rel} is the relative linear velocity, A_n is the nominal contact area, F_N is the normal force, P_a is the average power consumed by the actuator, which can be calculated from (1). Here, F_N/A_n represents the normal stress, and the product of friction and velocity is frictional energy. Therefore, the efficiency parameter can be interpreted as the amount of frictional energy saved with unit normal stress and unit power consumption.

In this study, normal loads were relatively small although the stress was achieved as high as 70 MPa. In real-world ultrasonic systems, the same level of stress might be reached, but with much higher forces and larger contact areas. It is assumed here that the efficiency coefficient of a certain stress remains its value as long as the stress is the same, even if both normal load and nominal contact area are at higher levels.

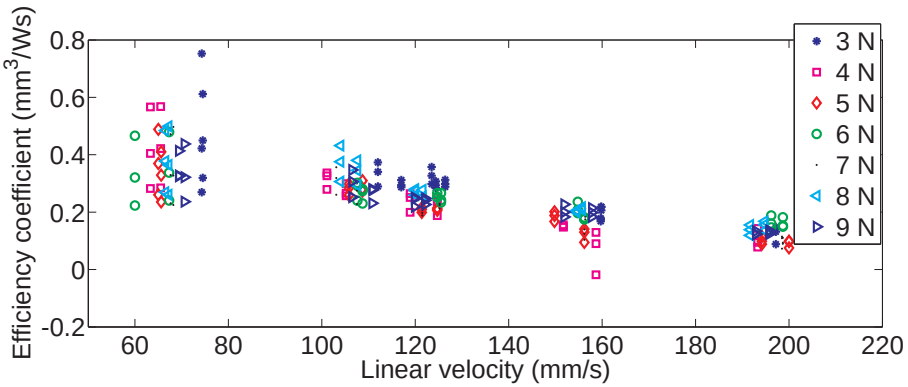

Figure 9. Relationship between efficiency coefficient and linear velocity.

Figure 9 plots the values of all the efficiency coefficients against linear velocity. Each marker represents the value derived from one measurement regardless of the conditions of normal stress or linear velocity. It is evident that markers concentrate at higher velocities and scatter at low velocity. The reason is that, at low velocities, there exists optimum power consumption. The extra power applied to the actuator does not result in any additional friction reduction, which leads to a drop in efficiency. Those markers should concentrate if the power used for calculation was at its optimum. Nevertheless, a linear relationship can be found between the efficiency coefficient and the velocity. This relationship can be expressed as

$$\eta = av_{rel} + b, \tag{4}$$

where a and b are the constants for the fitted line, which are equal to -2.93 and 0.672, respectively (v_{rel} in m/s). Therefore, the power required for reducing friction from F_{t0} to F_{t1} can be calculated as

$$P_a = \frac{(F_{t0} - F_{t1})v_{rel}A_n}{F_N(av_{rel} + b)}. \tag{5}$$

Similarly, the new (reduced) friction can be calculated as

$$F_{t0} = F_{t1} - \frac{F_N(av_{rel} + b)P_a}{v_{rel}A_n}. \tag{6}$$

The efficiency coefficient and equations (5) and (6) can be employed to realize ultrasonic friction control, which is to modulate friction between high and low by driving the actuator with different levels of power. It should be noted that the values of the metric and the constants of the equations are only measured for the experimental set-up in this study. Each ultrasonic lubrication system has its unique design and the metric values should be calibrated for each system. This is only one example of how metrics can be utilized.

6. CONCLUDING REMARKS

This paper reports experimental study of the relationship between friction reduction, power consumption, linear velocity, and normal stresses. Each test contains measurements of intrinsic friction and friction forces with ultrasonic vibrations applied. Five levels of voltages were applied to the piezoelectric actuator for electric power ranging from 0.21 to 5.31 W, while the normal stress and linear velocity vary from 23 to 70 MPa and 50 to 200 mm/s, respectively. Friction reduction near 100% can be achieved under certain conditions. Friction reduction increases as the power increases, but decreases when the linear velocity increases. The magnitude of normal load/stress has little influence on the effectiveness of ultrasonic lubrication. However, the vibration of the structure results in variation of friction reduction because the added weight changes the resonance of the structure. Contour plots of friction reduction, power consumption, normal stress and linear velocity were created. An efficiency coefficient was proposed to calculate the power requirements for a certain friction reduction or reduced friction for a given electric power.

ACKNOWLEDGMENTS

We wish to acknowledge the member organizations of the Smart Vehicle Concepts Center, a National Science Foundation Industry/University Cooperative Research Center (www.SmartVehicleCenter.org) established under NSF Grant IIP-1238286.

REFERENCES

[1] Bhushan, B., "Introduction to tribology," *John Wiley & Sons*, New York (2002).

[2] Graff, K., "Power ultrasonics: applications of high-intensity ultrasound," *Woodhead Publishing*, Cambridge (2014).

[3] Mason, W., "Physical acoustics and the properties of solids," *Van Nostrand,* Princeton (1958).

[4] Severdenko, V., Klubovich, V., and Stepanenko, A., "Ultrasonic rolling and drawing of metals, " *Consultants Bureau*, New York and London (1972).

[5] Littmann, W., Storck, H., and Wallaschek, J., "Sliding friction in the presence of ultrasonic oscillations: superposition of longitudinal oscillations," *Arch. Appl. Mech.*, **71,** 549-554 (2001).

[6] Kumar, V. and Hutchings, I., "Reduction of the sliding friction of metals by the application of longitudinal or transverse ultrasonic vibration," *Tribol. Int.*, **37**, 833-840 (2004).

[7] Popov, V., Starcevic, J., and Filippov, A., "Influence of ultrasonic in-plane oscillations on static and sliding friction and intrinsic length scale of dry friction processes," *Tribol. Lett.*, **39**, 25-30 (2010).

[8] Teidelt, E., Starcevic, J, and Popov, V., "Influence of ultrasonic oscillation on static and sliding friction, " *Tribol. Lett.*, **1**, 51-62 (2012).

[9] Gutowski, P. and Leus, M., "The effect of longitudinal tangential vibrations on friction and driving forces in sliding motion," *Tribol. Int.*, **55**, 108-118 (2012).

[10] Pohlman, R., Lehfeldt, E., "Influence of ultrasonic vibration on metallic friction," *Ultrasonics*, **4** (4), 178-185 (1966).

[11] Oiwa, T., "Friction control using ultrasonic oscillation for rolling-element linear-motion guide," *Rev. Sci. Instrum.*, **77**, 016-107 (2006).

[12] Tsai, C. and Tseng, C., "The effect of friction reduction in the presence of in-plane vibrations," *Arch. Appl. Mech.*, **75**, 164-176 (2005).

[13] Bharadwaj, S. and Dapino, M. J., "Effect of load on active friction control using ultrasonic vibrations," *Proc. SPIE*, **7290**, 72900G (2009).

[14] Bharadwaj, S. and Dapino, M. J., "Friction control in automotive seat belt systems by piezoelectrically generated ultrasonic vibrations," *Proc. SPIE*, **7645**, 76450E (2010).

[15] Bharadwaj, S. and Dapino, M. J., "Characterization of friction reduction with tangential ultrasonic vibrations using a SDOF model," *Inter. J. of Vehicle Des.*, **63** (2/3) (2013).

[16] Dong, S. and Dapino, M. J., "Piezoelectrically-induced ultrasonic lubrication by way of Poisson effect," *Proc. SPIE*, **8343L** (2012).

[17] Dong, S. and Dapino, M. J., "Elastic-plastic cube model for ultrasonic friction reduction via Poisson effect," *Ultrasonics*, **54**, 343-350 (2014).

[18] Dong, S. and Dapino, M. J., "Wear reduction through piezoelectrically-assisted ultrasonic lubrication," *Proc. ASME conference on SMASIS*, Snowbird, Utah (2013).

[19] Dong, S. and Dapino, M. J., "Wear reduction through piezoelectrically-assisted ultrasonic lubrication," *Smart. Mater. Struct.* **23**, 104005 (2014).

[20] Dong, S. and Dapino, M. J., "Model for friction and wear reduction through piezoelectrically-assisted ultrasonic lubrication," *Proc. SPIE*, **9059**, 90590C (2014).

[21] Uchino, K. "Piezoelectric ultrasonic motors: overview," *Smart. Mater. Struct.* **7**, 273-285(1998).